Appendix. "Keep the Water Flowing: The Hidden Crisis of Rural Water Management"

A. Afridev Handpumps: Design and Servicing

In this section, we delve into the design and maintenance of the Afridev handpumps, which are the most widely used type in Africa (Carter 2021). Our discussion draws from the Installation and Maintenance Manual (Erpf 2007), as well as the first author's field research in Malawi. During her time there, she assisted in two major repairs and two minor repairs.

The Afridev handpump's main above-ground components include the pump handle, pump head cover, pump head, and pump pedestal (which supports both above and below-ground components). The main underground components include pump rods (connected to the plunger for above-ground operation), a plunger (enabling suction and delivery of water), a foot-valve (allowing unidirectional water flow into the pipes), a cylinder (which draws and pumps water to the ground level), and rising main pipes (that carry water from the cylinder to the ground level). The Afridev handpump has an open-top cylinder design that allows for easy removal of the main underground components for maintenance without having to pull and dismantle the heavier rising main pipes (Erpf 2007). Afridev handpumps use plastics and rubber extensively, which are cheap but can wear out quickly, especially if they are of poor quality. There are six fast-wearing parts: bush bearing, U-seal, bobbin, O-ring, cup seal, and rod centralizer.

When a water point experiences a *minor* breakdown, it still provides water, but water may come out at a delayed or reduced water flow, or it may make abnormal noise during operation. A minor breakdown only requires the replacement of the spare parts. For example, delayed or reduced water flow can result from worn cup seals or a leak in the foot valve or plunger, in which case the mechanic needs to replace the worn bobbins and/or the O-rings. When a water point experiences a *major* breakdown, it does not provide any water, and it is caused by broken rising main pipes. Usually, if a minor breakdown is not addressed promptly, small parts can further fall into the rising main pipes, causing blockages and perforations over time. Bent pump rods can rub on the rising main pipes and may eventually perforate the pipes. Repairing the rising main pipes is very complex and requires at least eight people.

B. Water Points' Cascade Failure

When a water point breaks down, communities may walk to a nearby water point to get water, adding stress to the nearby water point and potentially leading to its failure as well. Although there is no available data on water usage at each water point, we analyzed longitudinal data on water points' functionality in Malawi to explore this cascade effect. We plotted the functionality status over time of two water points within a one-kilometer distance from each other (and with no other water points within that distance). We find some scattered evidence of the cascade effect. One example is of two water points located 565 meters apart: on July 22, 2020, the *focal water point* first experienced a minor breakdown, while the *nearby water point* was still functional. About five months later, on January 13, 2021, the *nearby water point* experienced a minor breakdown itself. In the same month, the *focal water point* was found to be functional on January 26, 2021. Then on April 29, 2021, the *focal water point* was found to need a minor repair again, meanwhile the *nearby water point* was still needing a minor repair. Finally on February 22, 2022, the *nearby water point* needed a major repair.

We observed similar patterns of cascade failures on 23 pairs of water points. The mechanics' notes also provided indications of such behavior. We quote two of them below: "the surrounding borehole has just stopped working so the number of families using this water point has raised up.they need a help on borehole maintenance." "It is working but it's two surrounding boreholes are not working. This has been forcing this borehole to be in use day and night.in future this will cause a very big problem to this borehole."

C. Data and Implementation

This section details the data cleaning procedures in Malawi, CAR, and Ethiopia. When visiting each water point or calling each community, the NGO mechanic fills out a survey using a tablet. Each NGO uses a different survey and database. While the NGO mechanics in each country were trained on how to accurately

complete the survey, errors still occur. There were also duplicated records due to app freezing or unstable internet connections. To address the potential human and technical errors, we collaborated with our NGO partners to clean the data. Their expertise proved invaluable in identifying and correcting human errors, and interpreting the data accurately.

C.1. Kaplan-Meier Estimator

Figure A.1 presents the estimated probability of breakdown in Malawi (as well as Ethiopia and CAR) after a specific number of months from the previous service. To verify that our K-M estimates reflect an underlying process independent of visitation policies and are generalizable beyond our sample, we perform temporal splits and k-fold cross-validation. Complete results for both validation strategies are provided in Table A.1. Our findings show that, across all temporal splits and all but one cross-validation fold, the log-rank test yields a p-value greater than 0.05, indicating no statistically significant difference between the K-M curves at the 0.05 level.

Figure A.1 The estimated probability of breakdown in the three countries (with only 8 months of pre-civil war data available from Ethiopia)

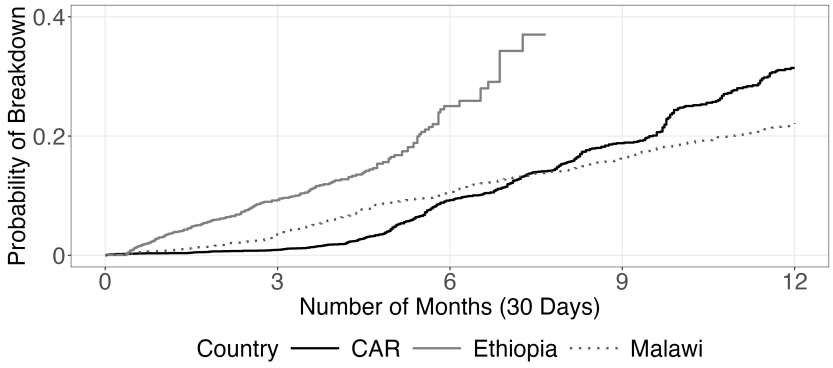

For temporal split, in Berbérati and Bangui (CAR), we use data from 2018–2021 for training and data from 2022 for testing; in Malawi, training data is from 2019–2021 and test data from 2022; in Ethiopia, due to the 2021 conflict in Tigray, we use 2020 as training and 2022 as test data. For each region, we fit K-M estimators separately for the training and test sets and then apply a log-rank test to assess whether the time-to-breakdown distributions differ between the training and the test periods. For grouped k-fold cross-validation, we set $k = 3, 6, 9, 12$, and 15, partitioning the data at the water point level to ensure that all observations from a given water point remain within the same fold. For each split, we fit a K-M curve on the $k-1$ training folds and another on the held-out fold, then use the log-rank test to compare the resulting survival distributions. We vary the value of k to examine the stability and robustness of our estimates: smaller k values yield larger test sets and higher bias, while larger k values reduce bias but increase variance. To combine the k resulting p-values, we compute the harmonic mean p-value, which is well-suited for combining dependent tests such as those arising in cross-validation, where the same water point may contribute to multiple folds (Wilson 2019). We additionally report the percentage of folds with $p > 0.05$ and the median p-value across folds.

C.2. Malawi

Fisherman's Rest has been operating in TA Somba since its establishment in 2013. Since 2018, the NGO has gradually expanded its program to include additional TAs: TA Kunthembwe and Kuntaja in 2019, TA Kapeni, Machinjiri, and Makata in 2020, and TA Chigaru and Lundu in 2021. We apply the K-means clustering algorithm to divide the 201 water points in TA Somba into four clusters, shown in Figure A.2.

Table A.1 Log-rank test results (p-values). $p > 0.05$ indicate no statistically significant difference.

Region	Temporal	Cross-Validation Metric	$k=3$	$k=6$	$k=9$	$k=12$	$k=15$
Berbérati	0.087	Harmonic mean p	0.752	0.801	0.611	0.843	0.778
		# $p > 0.05$	3/3	6/6	9/9	12/12	15/15
		Median p	0.780	0.687	0.420	0.735	0.579
Bangui	0.180	Harmonic mean p	0.633	0.304	0.451	0.564	0.069
		# $p > 0.05$	3/3	6/6	9/9	12/12	14/15
		Median p	0.528	0.520	0.399	0.582	0.253
Ethiopia	0.063	Harmonic mean p	0.728	0.728	0.795	0.784	0.614
		# $p > 0.05$	3/3	6/6	9/9	12/12	15/15
		Median p	0.615	0.517	0.542	0.605	0.599
Malawi	0.644	Harmonic mean p	0.711	0.321	0.567	0.670	0.741
		# $p > 0.05$	3/3	6/6	9/9	12/12	15/15
		Median p	0.690	0.269	0.417	0.447	0.486

C.2.1. Data Cleaning The raw data from Malawi include 18,664 records from January 2010 to December 2022. The data collected through each call and visit includes the water point's functionality, communities' past efforts to repair it, and detailed but unstructured comments from NGO staff. Only 12.2% of the records are from 2010-2018, and the *Madzi Alipo* program did not start systematically collecting data until 2019.

SurveyType refers to the type of survey: *Repair* (an actual visit by a mechanic to repair a water point in the field), *CallOutgoing* (when the NGO calls a community to gather information), *CallIncoming* (when a community contacts the NGO for assistance, which is extremely rare), *PartPurchase* (when a community contacts the NGO to purchase spare parts), *BalanceInquiries* (when the NGO provides loans to communities to purchase spare parts), and *SensorOnlyVisits* (when the NGO installs sensors on water points in the field).

Status indicates the functionality status of the water points when the mechanic arrived: *Not Working* (i.e., *Major*), *Working but requires servicing* (i.e., *Minor*), and *Working* (i.e., *Functional*). We remove the records with unknown status and the abandoned water points. There are 781 cases categorized as both repairs and as functional, which is inconsistent. Further investigation reveals that 368 of these cases were actually site visits to install sensors. Thus, we modify their *SurveyType* to *SensorOnlyVisits*. For the remaining 413 cases, information is available regarding the parts used in the repair. Based on our conversations with the NGO, a major repair requires new rising main pipes, stainless steel rods, and/or a cylinder. Therefore, we reclassify the *Status* of the repairs that used these parts as *Major* and the rest as *Minor*.

We remove duplicated records by first renaming the duplicated visit ID. Per NGO's instruction, for water points with two records on the same day, if the records had different *SurveyType*, we keep the record that is a *Repair*. If none of the records was a *Repair*, we keep the *CallOutgoing* record. If none was *Repair* or *CallOutgoing*, we keep the *PartsPurchase* record. If none was *Repair*, *CallOutgoing*, or *PartsPurchase*, we keep the *CallIncoming* record. After the above data cleaning process, there are 14,839 records from 2019 to 2022.

Figure A.2 A map of the 4 clusters in TA Somba in Malawi

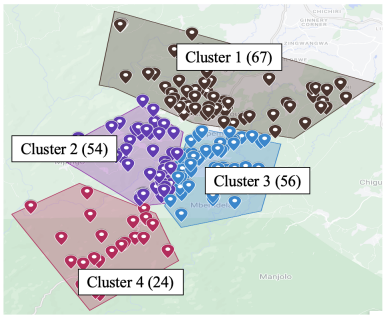

C.2.2. Robustness Checks In this section, we provide additional analysis to show the robustness of our results. First, Table A.2 provides the results from TA Somba in 2022 (post-COVID). When adhering to a cluster visitation schedule aligned with current practices, water point downtime increases by 722 days. This increase is likely due to the inflexibility of cluster visits, whereas the current day tour approach allows for quicker responses to recently broken water points in other clusters. Nevertheless, incorporating preventive maintenance with an optimized cluster visitation schedule, compared to current practices (Column B), can reduce downtime by 709 days (8.6%) and logistics cost by $1,648 (27.7%). Column (E), which assumes two water points per day, increases travel costs but still reduces logistics costs by $1,548 compared to Column (B). From the lower and upper K-M bounds, we find the reduction in downtime ranges from 4.0% to 16.2%, and the reduction in logistics cost ranges from 24.0% to 31.9%.

Table A.2 Results from TA Somba in 2022 of 272 water points (with K–M bounds)

	(A)	(B)	(C)	(D)	(E)	Lower		Upper	
	Reported	$\tilde{p}(\Delta)$	With Preventive Maintenance	MDP		$\tilde{p}(\Delta)$	MDP	$\tilde{p}(\Delta)$	MDP
				One Tour	2WP/Day				
Downtime	7,595	8,203	8,925	7,494		7,411	7,112	9,382	7,858
# Major	78	77	34	17		67	14	89	20
# Minor	99	100	196	261		110	264	88	258
Travel Distance	492	492	154	164	1,512	492	164	492	164
Logistics Cost ($)	6,001	5,953	4,522	4,305	4,405	5,472	4,161	6,530	4,449
Parts Cost ($)	5,964	5,916	4,510	4,293	4,293	5,435	4,148	6,493	4,437
(% of total)	(99.38%)	(99.38%)	(99.73%)	(99.72%)	(97.46%)	(99.32%)	(99.69%)	(99.43%)	(99.73%)
Travel Cost ($)	37	37	12	12	112	37	13	37	12
(% of total)	(0.62%)	(0.62%)	(0.27%)	(0.28%)	(2.54%)	(0.68%)	(0.31%)	(0.57%)	(0.27%)

Note: From column (B) to (D), logistics cost decreases by $1,648, of which $1,623 (98.5%) comes from lower parts costs and $25 (1.5%) comes from reduced travel distance.

Second, we extend our analysis to cover the entire Blantyre district in both 2019 and 2022, with results presented in Tables A.3 and A.4. In 2022, the NGO managed 1,502 water points (vs. 728 in 2019), and the communities (or some other unknown organizations) conducted 179 major repairs (vs. 56 in 2019) and 410 minor repairs (vs. 97 in 2019). In 2019, the optimization model reduces downtime by 21,629 days (52.7%) and logistics cost by $2,308 (16.3%), requiring an additional 277 water point visits. In contrast, in 2022, the optimization model reduces downtime by 3,642 days (7.1%) and logistics cost by $2,312 (9.1%), requiring an additional 448 water point visits. Similarly to the case of TA Somba, we observe a reduction in the benefit of the optimization model from 2019 to 2022, which could be attributed to the impact of the training program. Under the assumption of visiting two water points per day (Column E), logistics cost is reduced by $1,127 in 2019, and increased by $837 in 2022. The increase in travel distance is more pronounced in the two Blantyre cases than in TA Somba because the district-wide scope of the analysis includes many water points located far from the NGO office. In contrast, in TA Somba the office is located within the study area.

Finally, Tables A.3 and A.4 provides the results from the Blantyre district using the lower and upper bounds of K-M estimate. In 2019, the reduction in downtime ranges from 53.2% to 54.2% and the reduction in logistics cost ranges from 14.0% to 20.5%. In 2022, the reduction in downtime ranges from 6.3% to 13.6% and the reduction in logistics cost ranges from 0.2% to 18.3%.

C.3. CAR

Water for Good operates out of two base camps, one in Berbérati and one in Bangui in western CAR. The NGO divides the 2,348 water points under its management in rural areas into 55 groups known as "missions." There are four mechanic teams responsible for rural areas, with two operating out of each base camp. The data span from January 2018 to December 2022. Each entry is associated with a unique water point ID, date, mechanic team ID, and longitude and latitude of the water point. Additionally, the survey provides information including water point functionality upon arrival and departure, service required, and handpump type. For water point status upon arrival and departure, the survey provides three possible answers: 'yes' (functional), 'problem' (requiring minor repair), and 'no' (not functional and needing major repair). To clean the data, we first remove duplicated records, which are multiple visits to the same water point on the

Table A.3 Blantyre District results in 2019 (728 water points)

	(A) Reported	(B) $\tilde{p}(\Delta)$	(C) With Preventive Maintenance	(D) MDP One Tour	(E) MDP 2WP/Day	Lower $\tilde{p}(\Delta)$	Lower MDP	Upper $\tilde{p}(\Delta)$	Upper MDP
Downtime	40,042	41,060	29,811	19,431		39,098	17,902	44,102	20,634
# Major	197	173	122	60		159	56	188	58
# Minor	237	261	504	651		275	650	246	664
Travel Distance	5,779	5,779	1,237	1,257	17,213	5,779	1,273	5,779	1,263
Logistics Cost ($)	15,328	14,174	13,785	11,867	13,047	13,501	11,613	14,895	11,908
Parts Cost ($)	14,901	13,746	13,693	11,774	11,774	13,073	11,519	14,468	11,815
(% of total)	(97.21%)	(96.98%)	(99.48%)	(99.22%)	(90.24%)	(96.83%)	(99.19%)	(97.13%)	(99.22%)
Travel Cost ($)	427	428	92	93	1,273	428	94	427	93
(% of total)	(2.79%)	(3.02%)	(0.52%)	(0.78%)	(9.76%)	(3.17%)	(0.81%)	(2.87%)	(0.78%)

Note: From column (B) to (D), logistics cost decreases by $2,307, of which $1,972 (85.5%) is from lower parts costs and $335 (14.5%) is from reduced travel distance.

Table A.4 Blantyre District results in 2022 (1,502 water points)

	(A) Reported	(B) $\tilde{p}(\Delta)$	(C) With Preventive Maintenance	(D) MDP One Tour	(E) MDP 2WP/Day	Lower $\tilde{p}(\Delta)$	Lower MDP	Upper $\tilde{p}(\Delta)$	Upper MDP
Downtime	51,835	51,234	56,017	47,592		47,519	44,512	57,667	49,855
# Major	307	313	179	134		273	148	353	114
# Minor	490	484	989	1,186		524	1,145	444	1,223
Travel Distance	5,147	5,147	1,828	1,911	44,464	5,147	1,894	5,147	1,905
Logistics Cost	25,110	25,399	23,345	23,087	26,236	23,475	23,421	27,323	22,337
Parts Cost ($)	24,729	25,018	23,210	22,945	22,945	23,094	23,281	26,942	22,196
(% of total)	(98.48%)	(98.50%)	(99.42%)	(99.38%)	(87.46%)	(98.38%)	(99.40%)	(98.61%)	(99.37%)
Travel Cost ($)	381	382	135	142	3,291	380	139	379	140
(% of total)	(1.52%)	(1.50%)	(0.58%)	(0.62%)	(12.54%)	(1.62%)	(0.60%)	(1.39%)	(0.63%)

Note: From column (B) to (D), logistics cost decreases by $2,312, of which $2,073 (89.7%) is from lower parts costs and $239 (10.3%) is from reduced travel distance.

same day by retaining records with the worst functionality upon arrival. If duplicated records have the same functionality upon arrival, we keep the visit record with the most complete data. After cleaning, the data comprises 14,817 unique visit records.

C.3.1. Kaplan-Meier Estimator in CAR In the case of CAR, we analyze all available data from 2018 onwards, the year that the NGO expanded its operations in the country. In Figure A.3, we plot the K-M probability of breakdown (i.e., 1 - survival rate) for water points in the Berbérati area and the Bangui area, along with the corresponding 95% confidence interval between the two areas. We find that there is a significant difference in the survival curve. This is further confirmed by a log-rank test, with the null hypothesis that there is no difference between the water points in the probability of an event (i.e., a breakdown) at any time point. The log-rank test shows a p-value of $3e-12$. Thus, we use different probability of breakdown when applying the optimization model to the Berbérati area and the Bangui area.

C.3.2. Robustness Checks Table A.5 provides the results from Bangui in 2022. The NGO missed 270 visits to 199 water points, and did not conduct preventive maintenance service on 220 water points. Incorporating preventive maintenance with optimized cluster visitation schedule demonstrates the potential to reduce water point downtime by 6,216 days (41.7%) at an increase of logistics cost by $4,289 (18.8%). At the lower bound of the K-M estimate, the MDP reduces downtime by 6,897 days (50.8%) at an increase of logistics cost by $3,988 (18.0%). At the upper bound of the K-M estimate, the MDP reduces downtime by 6,773 days (41.7%) at an increase of logistics cost by $4,000 (17.1%).

C.3.3. Budget Constraint In this section, we formulate a MDP in which we minimize downtime subject to a budget constraint. We consider a finite-horizon planning problem over 12 periods (i.e., one year) with a limited total budget. To incorporate the budget constraint, we introduce a new state variable ϕ_t that tracks the remaining budget at time t. The dynamic programming problem is solved via backward induction, from the terminal period (when no future cost is incurred) back to the first period. Define the system state at time t as $\mathbf{s}_t = \big(\Omega_t, \Delta_t, \phi_t\big)$, where Ω_t is a vector of the percentage of reported broken water points across the

Figure A.3 Probability of breakdown using a Kaplan-Meier Estimator in Berbérati area vs. the Bangui area

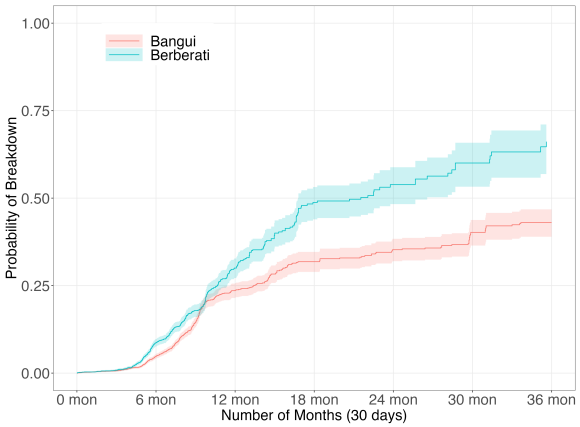

Table A.5 CAR results in the Bangui area in 2022 of 991 water points (with K–M bounds)

	(A)	(B)	(C)	(D)	Lower		Upper	
	Reported	$\tilde{p}(\Delta)$	With Preventive Maintenance	MDP	$\tilde{p}(\Delta)$	MDP	$\tilde{p}(\Delta)$	MDP
Downtime (Days)	12,437	14,914	12,581	8,698	13,572	6,675	16,239	9,466
# Major	164	156	181	110	143	91	169	117
# Minor/ Preventive	890	1,018	1,263	1,568	1,031	1,586	1,005	1,561
Travel Distance (km)	8,253	8,253	8,850	10,979	8,253	10,975	8,253	10,980
Logistics Cost ($)	21,674	22,789	27,411	27,078	22,164	26,152	23,415	27,415
Parts Cost ($)	21,063	22,179	26,756	26,266	21,553	25,340	22,804	26,603
(% of total)	(97.18%)	(97.32%)	(97.61%)	(97.00%)	(97.24%)	(96.90%)	(97.39%)	(97.04%)
Travel Cost ($)	611	610	655	812	601	812	611	812
(% of total)	(2.82%)	(2.68%)	(2.39%)	(3.00%)	(2.71%)	(3.10%)	(2.61%)	(2.96%)

Note: From column (B) to (D), logistics cost increases by $4,289, of which $4,087 (95.3%) is due to higher parts costs and $202 (4.7%) is due to increased travel distance.

N_c clusters, Δ_t is a vector of the period since the last visit across the N_c clusters, and ϕ_t is a vector of the remaining budget across the N_c clusters.

Let $g(\Omega_t, \Delta_t)$ be the total downtime incurred across all clusters during period t. Let $C((\Omega_t, \Delta_t), \mathbf{a}_t)$ be the logistics cost incurred in period t when action $\mathbf{a}_t$ is taken. The state transitions for Ω_t and Δ_t are the same as before. The budget transition is $\phi_{t+1} = \phi_t - C((\Omega_t, \Delta_t), \mathbf{a}_t)$. Define the value function $\nu^\star(\mathbf{s}, t)$ as the minimum expected total downtime achievable from period t to the terminal period T, starting from state $\mathbf{s}$. The Bellman recursion is: $\nu^\star(\mathbf{s}, t) = \min_{\{\mathbf{a}_\tau\}_{\tau=t}^T} \mathbb{E}\left[\sum_{\tau=t}^T \eta^{(\tau-t)}\, g\big(\mathbf{s}_\tau, \mathbf{a}_\tau\big) \middle| \mathbf{s}_t = \mathbf{s}\right]$ for $t = 1, 2, ..., T$, with the terminal condition $\nu^\star(\mathbf{s}, T+1) = 0, \forall \mathbf{s}$.

We apply the model to data from Berbérati and Bangui. In Berbérati, the minimum downtime without a budget constraint is 7,478 days, a 54.7% reduction compared to current practice. With the budget constraint, the minimum downtime increases to 8,249 days, still representing a 50.0% reduction. In Bangui, the minimum downtime without a budget constraint is 8,698 days, a 41.7% reduction compared to current practice. With the budget constraint, the minimum downtime increases to 9,129 days, corresponding to a 38.8% reduction.

C.4. Ethiopia

Relief Society of Tigray (*REST*) is a local grassroots NGO working in Tigray, Ethiopia since 1978. The NGO works in eight zones in the Tigray Region. In November 2020, a civil war started in Tigray. *REST* stopped its water point maintenance operations in many regions and focused on food and other humanitarian aid delivery.

C.4.1. Data Cleaning The raw data from Ethiopia includes 17,799 records of mechanics visiting water points from March 4, 2020 to August 29, 2022. Each record contains a unique water point ID, date of the visit, mechanic ID, and longitude and latitude of the water point. We first remove duplicated records where multiple visits were made to the same water point on the same day. We retain the visit record with the most complete data, leading to 17,584 unique mechanic visits. We create the variable ***Status*** to indicate the functionality status of the water points. Specifically, we analyze seven survey questions: (1) "What type of repair is needed at this water point?" (2) "Does the community use this water point to collect drinking water?" (3) "Why is the water point not in use?" (4) "What is the final status of the water point upon departure?" (5) "Why does the water point have low yield or no water available?" (6) "Does this water point require any repairs?" and (7) "Does this water point need preventative maintenance?" Not all fields are filled out. Based on the answers, we create seven levels of functionality status: *Functional*, *Minor*, *Major*, *Rehabilitation*, *PermanentDry*, and *NotInUse*.

C.4.2. Constructing Mechanic Tours and Clusters There are 549 water points in the Western Zone, with 62 of them not being actively used by the local communities due to reasons such as water points being permanently dry. Thus, in the numerical study in Section 6, we only look at the remaining 487 water points. To analyze current practices, we reconstruct mechanic tours by determining which mechanic(s) visited which water points on a tour using the steps below:

1. We began with the base tours, i.e., visits by a mechanic on consecutive days.
2. Each base tour was then investigated to determine whether two consecutive tours could be combined. Tours could be combined if the time gap between them was less than two days, they were not on opposite sides of the zone office, and the last day of the first tour and the first day of the second tour were geographically close together or along the same road.
3. Long tours of more than 21 days were investigated. They were divided into multiple smaller tours if the visits between two days were located on different sides of the zone office.
4. Sometimes multiple mechanics traveled together on the same tour and took turns filling out the survey. Thus, we combined the tours by these mechanics during the same period.

This process creates 86 mechanic tours. We find that mechanics sometimes conduct day tours, visiting only one or two water points located near the town where the NGO office is located. Mechanics go on longer tours lasting up to 21 days to visit the water points in rural areas. To account for this pattern, we separate the 89 water points near the office from the remainder. We then create five clusters with the remaining water points based on the reconstructed tours. The five clusters have 81, 68, 85, 83, and 81 water points.

C.4.3. Kaplan-Meier Estimator in Ethiopia Due to the civil war in Tigray from November 2020 to November 2022, the mechanics selectively visited the water points they could reach. They also started to visit water points that were not previously under their management. These changes could add significant bias into our data analysis. Therefore, when estimating the probability breakdown using the K-M estimator, we use only the data before November 1, 2020.

C.4.4. Robustness Checks We conduct a parallel analysis for the Seneale Zone in 2020 (Table A.6) and 2021 (Table A.7), pre-war and during the war. We find that in Seneale in 2020 (i.e., before the war started), incorporating preventive maintenance with optimized schedule could reduce water point downtime by 18,256 days (48.7%) and logistics cost by $1,051 (4.9%). At the lower bound of the K–M estimate, the MDP reduces downtime by 17,010 days (50.6%) at a decrease of logistics cost by $1,082 (5.2%). At the upper bound of the K–M estimate, the MDP reduces downtime by 18,549 days (45.1%) at an increase of logistics cost by $247 (1.1%). In 2021 (i.e., after the war started), the optimization model could reduce water point downtime by 33,297 days (61.9%) and logistics cost by $1,775 (6.3%). However, the NGO would need to conduct an additional 235 water point visits, which could be challenging due to the on-going war. At the lower bound of the K–M estimate, the MDP reduces downtime by 32,643 days (65.9%) at a decrease of logistics cost by $2,737 (10.0%). At the upper bound of the K–M estimate, the MDP reduces downtime by 33,756 days (58.5%) at a decrease of logistics cost by $812 (2.8%).

Table A.6 Ethiopia results in the Seneale Zone in 2020 of 625 water points (with K–M bounds)

	(A)	(B)	(C)	(D)	Lower		Upper	
	Reported	$\tilde{p}(\Delta)$	With Preventive Maintenance	MDP	$\tilde{p}(\Delta)$	MDP	$\tilde{p}(\Delta)$	MDP
Downtime (Days)	33,632	37,470	25,876	19,214	33,626	16,616	41,122	22,573
# Major	171	180	187	174	167	164	193	197
# Minor/Preventive	846	837	1,019	790	850	786	824	832
Travel Distance (km)	3,175	3,175	2,237	1,822	3,175	1,824	3,175	1,895
Logistics Cost ($)	21,173	21,605	24,235	20,554	20,980	19,898	22,231	22,478
Parts Cost ($)	20,938	21,371	24,070	20,419	20,745	19,763	21,996	22,338
(% of total)	(98.89%)	(98.92%)	(99.32%)	(99.34%)	(98.88%)	(99.32%)	(98.94%)	(99.38%)
Travel Cost ($)	235	234	165	135	235	135	235	140
(% of total)	(1.11%)	(1.08%)	(0.68%)	(0.66%)	(1.12%)	(0.68%)	(1.06%)	(0.62%)

Note: From column (B) to (D), logistics cost decreases by $1,051, of which $951 (90.5%) is due to lower parts costs and $100 (9.5%) is due to reduced travel distance.

Table A.7 Ethiopia results in the Seneale Zone in 2021 of 602 water points (with K–M bounds)

	(A)	(B)	(C)	(D)	Lower		Upper	
	Reported	$\tilde{p}(\Delta)$	With Preventive Maintenance	MDP	$\tilde{p}(\Delta)$	MDP	$\tilde{p}(\Delta)$	MDP
Downtime (Days)	55,180	53,765	28,999	20,468	49,576	16,933	57,684	23,928
# Major	324	307	209	210	293	176	320	243
# Minor/Preventive	714	731	1,227	1,064	745	1,098	718	1,031
Travel Distance (km)	3,208	3,208	2,517	2,409	3,208	2,410	3,208	2,410
Logistics Cost ($)	28,797	27,979	28,189	26,204	27,306	24,569	28,604	27,792
Parts Cost ($)	28,559	27,742	28,003	26,026	27,068	24,391	28,367	27,613
(% of total)	(99.27%)	(99.15%)	(99.34%)	(99.32%)	(99.13%)	(99.28%)	(99.17%)	(99.36%)
Travel Cost ($)	238	237	186	178	238	178	237	179
(% of total)	(0.83%)	(0.85%)	(0.66%)	(0.68%)	(0.87%)	(0.72%)	(0.83%)	(0.64%)

Note: From column (B) to (D), logistics cost decreases by $1,775, of which $1,716 (96.7%) is due to lower parts costs and $59 (3.3%) is due to reduced travel distance.

D. Model Related

D.1. Proof of Theorem 1

Part (a): Recall that in Equation 1, we defined $Pr(H=h) = \binom{W-\Omega_{it}}{h}(p(\Delta_{it})\cdot q)^h(1-p(\Delta_{it})\cdot q)^{W-\Omega_{it}-h}$, where H is the random variable that represents the number of newly reported broken water points in a period. Now let $F_H(W-\Omega, h, pq)$ be the cumulative distribution function of the binomial random variable H, where $W-\Omega$ is the number of remaining water points (i.e., trials), h is the number of newly reported broken water points (i.e., failures), and pq is the probability of a water point broken and being reported. Define $P(\Omega_{i,t+1}|\Omega_{it}, \Delta_{i,t+1})$ to be the probability of cluster i having $\Omega_{i,t+1}$ number of reported broken water points in period $t+1$ given the state in period t, corresponding to Equation 1. For better readability of the proof, we remove the subscript t in Ω_{it} and Δ_{it}. And we use Ω_i' to represent the number of reported broken water points in cluster i in the next period. Additionally, the per-period value function is $g(\mathbf{s}) = \sum_i \Omega_i + (W_i - \Omega_i)\cdot(1-q)\cdot p(\Delta_i)$.

Let us define $C_t(\mathbf{s}) = \min_{\mathbf{a}_t} V_t(\mathbf{s}, \mathbf{a}_t)$, which equals:

$$C_t(\mathbf{s}) = g(\mathbf{s}) + \eta\cdot\min\{ \sum_{\Omega_2'=\Omega_2}^{W}\sum_{\Omega_3'=\Omega_3}^{W} P(\Omega_2'|\Omega_2,\Delta_2)\cdot P(\Omega_3'|\Omega_3,\Delta_3)\cdot C_{t+1}((0,1,\Omega_2',\Delta_2+1,\Omega_3',\Delta_3+1)), \tag{A.1}$$

$$\sum_{\Omega_1'=0}^{W}\sum_{\Omega_3'=\Omega_3}^{W} P(\Omega_1'|0,\Delta_1=1)\cdot P(\Omega_3'|\Omega_3,\Delta_3)\cdot C_{t+1}((\Omega_1',2,0,1,\Omega_3',\Delta_3+1)), \tag{A.2}$$

$$\sum_{\Omega_1'=0}^{W}\sum_{\Omega_2'=\Omega_2}^{W} P(\Omega_1'|0,\Delta_1=1)\cdot P(\Omega_2'|\Omega_2,\Delta_2)\cdot C_{t+1}((\Omega_1',2,\Omega_2',\Delta_2+1,0,1))\} \tag{A.3}$$

Equations A.1, A.2, and A.3 correspond to the expected value in period t of visiting cluster 1, 2, and 3, respectively. Specifically, we prove that Equation A.1$-$A.2 >0, A.1$-$A.3 >0, and there exists a value $\tau\in[0,W]$ such that A.2$-$A.3 >0 when $\Omega_3\geq\tau$, and A.2$-$A.3 <0 when $\Omega_3<\tau$. For a road map of the proofs, we first prove that A.1$-$A.2 >0. In the proof, we first observe that A.2 is independent of Ω_2. Thus,

we only need to prove that when $\Omega_2 = W$, A.1$-$A.2 > 0 and that A.1 is monotonically non-increasing in Ω_2. The proof for A.1$-$A.3 > 0 is similar. To prove the existence of τ, we first note that A.3 is independent of Ω_3. Thus, we only need to prove that A.2 is monotonically increasing in the value of Ω_3.

In the proofs, we will use the following properties, which we prove below:

$$g((\Omega_1, \Delta_1, \Omega_2, \Delta_2, \Omega_3, \Delta_3)) - g((\Omega_1^\star, \Delta_1, \Omega_2, \Delta_2, \Omega_3, \Delta_3)) \geq 0, \forall\, \Omega_1 \geq \Omega_1^\star, \tag{A.4}$$

$$g((\Omega_1, \Delta_1, \Omega_2, \Delta_2, \Omega_3, \Delta_3)) - g((\Omega_1, \Delta_1^\star, \Omega_2, \Delta_2, \Omega_3, \Delta_3)) \geq 0, \forall\, \Delta_1 \geq \Delta_1^\star, \tag{A.5}$$

$$C_t((0, 1, W, \Delta_2, \Omega_3, \Delta_3)) - C_t((0, 1, \Omega_2, \Delta_2^\star, \Omega_3, \Delta_3)) \geq 0, \forall\, \Omega_2 \leq W, \tag{A.6}$$

$$C_t((0, 1, \Omega, \Delta_2, \Omega, \Delta_3)) - C_t((0, 1, \Omega, \Delta_2, \Omega, \Delta_3^\star)) > 0, \forall\, \Delta_3 > \Delta_3^\star. \tag{A.7}$$

Equation A.4 is because $(\Omega_1 - \Omega_1^\star) \cdot \Big(1 - (1-q) \cdot p(\Delta_1)\Big) \geq 0, \forall\, \Omega_1 \geq \Omega_1^\star$. Equation A.5 is because $(W - \Omega_1) \cdot (1-q) \cdot \Big[p(\Delta_1) - p(\Delta_1^\star)\Big] \geq 0, \forall\, \Delta_1 \geq \Delta_1^\star$.

Equation A.6 is true regardless of the relative value of Δ_2 and $\Delta_2^\star$. We prove Equation A.6 using induction. In the basis step, i.e., at terminal period T, using equations A.4 and A.5, we have:

$$C_T((0, 1, W, \Delta_2, \Omega_3, \Delta_3)) - C_T((0, 1, \Omega_2, \Delta_2^\star, \Omega_3, \Delta_3)) = g((0, 1, W, \Delta_2, \Omega_3, \Delta_3)) - g((0, 1, \Omega_2, \Delta_2^\star, \Omega_3, \Delta_3)) \geq 0.$$

In the induction step, assuming that $C_{t+1}((0, 1, W, \Delta_2, \Omega_3, \Delta_3)) - C_{t+1}((0, 1, \Omega_2, \Delta_2^\star, \Omega_3, \Delta_3)) \geq 0$,

$$\begin{aligned}
&C_t((0, 1, W, \Delta_2, \Omega_3, \Delta_3)) - C_t((0, 1, \Omega_2, \Delta_2^\star, \Omega_3, \Delta_3)) \\
&= g((0, 1, W, \Delta_2, \Omega_3, \Delta_3)) - g((0, 1, \Omega_2, \Delta_2^\star, \Omega_3, \Delta_3)) \\
&\quad + \min\{C_{t+1}((0, 1, W, \Delta_2 + 1, \Omega_3', \Delta_3 + 1)), C_{t+1}((\Omega_1', 2, 0, 1, \Omega_3', \Delta_3 + 1)), C_{t+1}((\Omega_1', 2, W, \Delta_2 + 1, 0, 1))\} \\
&\quad - \min\{C_{t+1}((0, 1, \Omega_2', \Delta_2^\star + 1, \Omega_3', \Delta_3 + 1)), C_{t+1}((\Omega_1', 2, 0, 1, \Omega_3', \Delta_3 + 1)), C_{t+1}((\Omega_1', 2, \Omega_2', \Delta_2^\star + 1, 0, 1))\} \\
&\geq C_{t+1}((\Omega_1', 2, 0, 1, \Omega_3', \Delta_3 + 1)) \\
&\quad - \min\{C_{t+1}((0, 1, \Omega_2', \Delta_2^\star + 1, \Omega_3', \Delta_3 + 1)), C_{t+1}((\Omega_1', 2, 0, 1, \Omega_3', \Delta_3 + 1)), C_{t+1}((\Omega_1', 2, \Omega_2', \Delta_2^\star + 1, 0, 1))\} \\
&= B - \min\{A, B, C\} \geq 0
\end{aligned}$$

The first inequality is because $g((0, 1, W, \Delta_2, \Omega_3, \Delta_3)) - g((0, 1, \Omega_2, \Delta_2^\star, \Omega_3, \Delta_3)) \geq 0$, proven in equation A.4. The first inequality also uses the induction hypothesis. For the last inequality, regardless of the value of $\min\{A, B, C\}$, $B - \min\{A, B, C\} \geq 0$. Thus we have concluded the proof for A.6.

We prove Equation A.7 using induction. In the basis step, i.e., at terminal period T, using the property of the per-period value function (g) proved in equation A.5, we have

$$C_T((0, 1, \Omega, \Delta_2, \Omega, \Delta_3)) - C_T((0, 1, \Omega, \Delta_2, \Omega, \Delta_3^\star)) = g((0, 1, \Omega, \Delta_2, \Omega, \Delta_3)) - g((0, 1, \Omega, \Delta_2, \Omega, \Delta_3^\star)) > 0$$

In the induction step, assuming that $C_{t+1}((0, 1, \Omega, \Delta_2, \Omega, \Delta_3)) > C_{t+1}((0, 1, \Omega, \Delta_2, \Omega, \Delta_3^\star)), \forall\, \Delta_3 > \Delta_3^\star$, we have:

$$\begin{aligned}
&C_t((0, 1, \Omega, \Delta_2, \Omega, \Delta_3)) - C_t((0, 1, \Omega, \Delta_2, \Omega, \Delta_3^\star)) \\
&= g((0, 1, \Omega, \Delta_2, \Omega, \Delta_3)) - g((0, 1, \Omega, \Delta_2, \Omega, \Delta_3^\star)) \\
&\quad + \min\{C_{t+1}((0, 1, \Omega', \Delta_2 + 1, \Omega', \Delta_3 + 1)), C_{t+1}((\Omega_1', 2, 0, 1, \Omega', \Delta_3 + 1)), C_{t+1}((\Omega_1', 2, \Omega', \Delta_2 + 1, 0, 1))\} \\
&\quad - \min\{C_{t+1}((0, 1, \Omega', \Delta_2 + 1, \Omega', \Delta_3^\star + 1)), C_{t+1}((\Omega_1', 2, 0, 1, \Omega', \Delta_3^\star + 1)), C_{t+1}((\Omega_1', 2, \Omega', \Delta_2 + 1, 0, 1))\} \\
&> \min\{C_{t+1}((0, 1, \Omega', \Delta_2 + 1, \Omega', \Delta_3 + 1)), C_{t+1}((\Omega_1', 2, 0, 1, \Omega', \Delta_3 + 1))\} - \min\{C_{t+1}((0, 1, \Omega', \Delta_2 + 1, \Omega', \Delta_3^\star + 1)), C_{t+1}((\Omega_1', 2, 0, 1, \Omega', \Delta_3^\star + 1))\} \\
&= \min\{A, B\} - \min\{C, D\} > 0
\end{aligned}$$

The first inequality is because of equation A.5. Additionally the third element in each $\min\{\}$ is larger than the second element. For example, $C_{t+1}((\Omega_1', 2, \Omega', \Delta_2 + 1, 0, 1)) > C_{t+1}((\Omega_1', 2, 0, 1, \Omega', \Delta_3 + 1))$ because $\Delta_2 > \Delta_3$ and we can apply the induction hypothesis. For $\min\{A, B\} - \min\{C, D\}$, we know that $A > C$ and $B > D$ because of the induction hypothesis. There are four cases of the last equality and we show that they are all > 0. $\min\{A, B\} - \min\{C, D\}$ can equal: (1) $A - C > 0$; (2) $A - D$ because we have $A < B$, $D < C$, $A > C$ and $B > D$, i.e., $D < C < A < B$; (3) $B - C > 0$ because have $B < A$, $C < D$, $A > C$ and $B > D$, i.e., $C < D < B < A$; (4) $B - D > 0$. Thus we have concluded the proof for A.7.

Proof of A.1−A.2 >0.

$$A.1-A.2=\sum_{\Omega_3'=\Omega_3}^{W}P(\Omega_3'|\Omega_3,\Delta_3)\cdot\Big[\sum_{\Omega_2'=\Omega_2}^{W}P(\Omega_2'|\Omega_2,\Delta_2)\cdot C_{t+1}((0,1,\Omega_2',\Delta_2+1,\Omega_3',\Delta_3+1))-\sum_{\Omega_1'=0}^{W}P(\Omega_1'|0,\Delta_1=1)\cdot C_{t+1}((\Omega_1',2,0,1,\Omega_3',\Delta_3+1)$$

$$\text{When } \Omega_2=W,\ A.1-A.2=\sum_{\Omega_3'=\Omega_3}^{W}P(\Omega_3'|\Omega_3,\Delta_3)\cdot\Big[C_{t+1}((0,1,W,\Delta_2+1,\Omega_3',\Delta_3+1))-\sum_{\Omega_1'=0}^{W}P(\Omega_1'|0,\Delta_1=1)\cdot C_{t+1}((\Omega_1',2,0,1,\Omega_3',\Delta_3+1))\Big]$$

$$=\sum_{\Omega_3'=\Omega_3}^{W}\sum_{\Omega_1'=0}^{W}P(\Omega_3'|\Omega_3,\Delta_3)\cdot P(\Omega_1'|0,\Delta_1=1)\cdot\Big[C_{t+1}((0,1,W,\Delta_2+1,\Omega_3',\Delta_3+1))-((\Omega_1',2,0,1,\Omega_3',\Delta_3+1))\Big]>0$$

In the first equality, we substitute Ω_2 with W. The second equality is because $C_{t+1}((0,1,W,\Delta_2+1,\Omega_3',\Delta_3+1))$ is not dependent of Ω_1'. The last inequality, i.e., $C_{t+1}((0,1,W,\Delta_2+1,\Omega_3',\Delta_3+1))-C_{t+1}((\Omega_1',2,0,1,\Omega_3',\Delta_3+1))>0$, is because of Equation A.6. Thus, we have proven that when $\Omega_2=W$, A.1−A.2 >0. We now prove that A.1 is monotonically non-increasing in Ω_2. The difference in the value of $A.1$ between $\Omega_2=k+1$ and $\Omega_2=k$ for an arbitrary $0\le k<W$ equals:

$$\sum_{\Omega_3'=\Omega_3}^{W}P(\Omega_3'|\Omega_3,\Delta_3)\cdot\Big[\sum_{\Omega_2'=k+1}^{W}P(\Omega_2'|k+1)\cdot C_{t+1}((0,1,\Omega_2',\Delta_2+1,\Omega_3',\Delta_3+1))-\sum_{\Omega_2'=k}^{W}P(\Omega_2'|k)\cdot C_{t+1}((0,1,\Omega_2',\Delta_2+1,\Omega_3',\Delta_3+1))\Big]$$

$$=\sum_{\Omega_3'=\Omega_3}^{W}P(\Omega_3'|\Omega_3,\Delta_3)\sum_{\Omega_2'=k}^{W}C_{t+1}((0,1,\Omega_2',\Delta_2+1,\Omega_3',\Delta_3+1))\cdot\Big[P(\Omega_2'|k+1)-P(\Omega_2'|k)\Big]$$

$$\le\sum_{\Omega_3'=\Omega_3}^{W}P(\Omega_3'|\Omega_3,\Delta_3)\cdot C_{t+1}((0,1,W,\Delta_2+1,\Omega_3',\Delta_3+1))\cdot\sum_{\Omega_2'=k}^{W}\Big[P(\Omega_2'|k+1)-P(\Omega_2'|k)\Big]$$

$$=\sum_{\Omega_3'=\Omega_3}^{W}P(\Omega_3'|\Omega_3,\Delta_3)\cdot C_{t+1}((0,1,0,\Delta_2+1,\Omega_3',\Delta_3+1))\cdot\Big[F_H(W-h+1,W-h+1,pq)-F_H(W-h,W-h,pq))\Big]=0$$

The first inequality uses the more general form equation A.6. Thus we have proven that A.1−A.2 >0 by utilizing the property that A.2 is independent of Ω_2 and by proving that when $\Omega_2=W$, A.1−A.2 >0 and A.1 is monotonically non-increasing in Ω_2.

The proof for A.1−A.3 >0 is similar. Thus, we omit it here.

Proof of A.2−A.3 >0 when $\Omega_3\ge\tau$, and A.2−A.3 <0 when $\Omega_3<\tau$.

First note that Equation A.3 is independent of Ω_3. Thus, to prove the existence of τ, we only need to prove that Equation A.2 is monotonically non-decreasing in the value of Ω_3. This proof is very similar to the proof of A.1 being monotonically non-increasing in Ω_2. We now have proven that Equation A.1−A.2 >0, A.1−A.3 >0, and A.2−A.3 >0 when $\Omega_3\ge\tau$, and A.2−A.3 <0 when $\Omega_3<\tau$, concluding the proof of part (a).

Part (b): We can prove that A.3 is monotonically non-decreasing in the value of Ω_2, using a similar proof for proving A.1 is monotonically non-increasing in the value of Ω_2 and A.2 is monotonically non-decreasing in the value of Ω_3. Because A.2 is monotonically non-decreasing in the value of Ω_3, A.2 will equal to the value of A.3 at a larger Ω_3 value when Ω_2 is larger, i.e., the threshold τ is non-decreasing in the value Ω_2.

Part (c): Because A.2 is monotonically non-decreasing in the value of Ω_3, to prove that the threshold value is always larger than Ω_2, we only need to prove that A.2−A.3 <0 when $\Omega_2=\Omega_3=k$. Let $\Omega'=\Omega_2'=\Omega_3'$. We have:

$$A.2-A.3=\sum_{\Omega_1'=0}^{W}\sum_{\Omega'=k}^{W}P(\Omega_1'|0,\Delta_1=1)\cdot\Big[P(\Omega'|k,\Delta_3)\cdot C_{t+1}((\Omega_1',2,0,1,\Omega',\Delta_3+1))-P(\Omega'|k,\Delta_2)\cdot C_{t+1}((\Omega_1',2,\Omega',\Delta_2+1,0,1))\Big]$$

$$<\sum_{\Omega_1'=0}^{W}\sum_{\Omega'=k}^{W}P(\Omega_1'|0,\Delta_1=1)\cdot\Big[P(\Omega'|k,\Delta_3)\cdot C_{t+1}((\Omega_1',2,0,1,\Omega',\Delta_2+1))-P(\Omega'|k,\Delta_2)\cdot C_{t+1}((\Omega_1',2,\Omega',\Delta_2+1,0,1))\Big]$$

$$\le\sum_{\Omega_1'=0}^{W}P(\Omega_1'|0,\Delta_1=1)\cdot C_{t+1}((\Omega_1',2,W,\Delta_2+1,0,1))\cdot\sum_{\Omega'=k}^{W}\Big[P(\Omega'|k,\Delta_3)-P(\Omega'|k,\Delta_2)\Big]$$

$$=\sum_{\Omega_1'=0}^{W}P(\Omega_1'|0,\Delta_1=1)\cdot C_{t+1}((\Omega_1',2,W,\Delta_2+1,0,1))\cdot\Big[F_H(W-k,k-1,p(\Delta_2)q)-F_H(W-k,k-1,p(\Delta_3)q)\Big]=0$$

The first equality is because of equation A.7. The second inequality is from Equation A.6. □

D.2. Incorporate Communities' Ability to Repair Broken Water Points

We assume that if communities know how to do repairs, they will do so in the same period; if they do not know how to do repairs, they will never do it. The sequence of events at period t is the following: the NGO observes the state of each cluster i, $s_{it} = (\Omega_{it}, \Delta_{it})$ at the beginning of t. New breakdowns happen. With probability β, a new breakdown is repaired by the communities themselves because they know how to do it. After communities' repairs, the NGO will conduct visits to one cluster and conduct all necessary maintenance and repair activities. After all the visits are completed, the cluster that was not visited in period t will report any new and un-repaired major breakdowns with probability q. We assume that all the repairs, whether by communities or by NGO, happen toward the end of the period. Thus, all water points that are broken in period t will incur downtime for the entire period.

$$\Omega_{i,t+1} = (\Omega_{it} + \tilde{h}) \cdot (1 - a_{it})$$
$$\text{with } Pr(H = h) = \binom{W_i - \Omega_{it}}{h} (p(\Delta_{it}) \cdot q)^h (1 - p(\Delta_{it}) \cdot q)^{W_i - \Omega_{it} - h}, \text{ and } \Pr(\tilde{H} = \tilde{h} \mid H = h) = \binom{h}{\tilde{h}} (1-\beta)^{\tilde{h}} \beta^{h - \tilde{h}},$$
$$\Delta_{i,t+1} = \Delta_{it} \cdot (1 - a_{it}) + 1.$$

The per-period cost function is the same from the original formulation (Equation 3). To examine the impact of community repair capacity (β) on water point downtime, we conduct a numerical study using generated data of $N_c = 4$ clusters, each containing $W_i = 10$ water points. Figure A.4 illustrates that increasing β consistently reduces water point downtime across all values of b. When b is small, indicating high water point repair demand relative to NGO capacity, even modest increases in β yield substantial gains.

Figure A.4 The distribution of water point downtime as b and β increases.

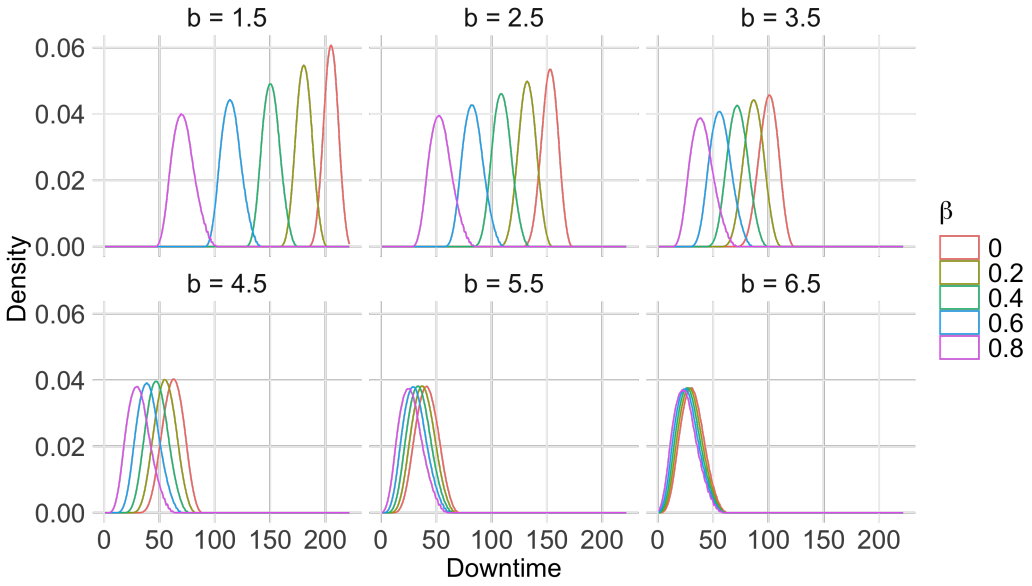

D.3. Reactive vs. Cyclic Visitation Approaches

In Section 5.3, we compared the performance of the cyclic and reactive maintenance visitation approaches. This section provides a more detailed discussion of those findings.

Under low information availability ($0.1 \leq q \leq 0.2$), we find that 94.8% of initial states have less than a 1% performance difference between the cyclic and reactive approaches. In other words, when functionality information is limited, the two approaches perform similarly.

Table A.8 further presents, under varying levels of functionality information availability, the percentage of initial states where the cyclic approach outperforms the reactive approach. Here we consider $q \in [0.3, 0.6]$ to be of medium information availability, and $q \in [0.7, 0.9]$ to be of high information availability. Overall, the relative effectiveness of each approach depends primarily on the balance between repair demand and NGO

capacity. When repair demand is high relative to capacity ($b < 3$, i.e., $b < N_c$), the cyclic approach tends to perform better. As repair demand decreases relative to capacity ($b > 4$, i.e., $b > N_c$), the reactive approach becomes more effective. While the level of functionality information influences performance, these trends remain consistent across different values of q.

We can further distinguish between likely and unlikely initial states. A likely initial state occurs when the cluster with a longer time since last visit (Δ) also has more reported breakdowns (Ω). In contrast, an unlikely initial state arises when a cluster with a shorter time since last visit has more reported breakdowns. Such situations may occur, for example, when NGOs resume operations after a disruption (e.g., post-conflict in Ethiopia), and some clusters have accumulated a disproportionate number of known breakdowns. Across the full parameter space (all values of a, b, and q), we find that in 72.4% of unlikely initial states, the reactive approach yields better performance. This advantage becomes even more pronounced when $b \geq 4.5$, where reactive visitation outperforms cyclic in 96.4% of cases. Based on these findings, we recommend that NGOs beginning from an unlikely initial state adopt a reactive visitation approach initially. As operations stabilize and the system transitions to a likely initial state, the NGO can shift to follow the policies recommended for those conditions.

Table A.8 Percentage of initial states where the cyclic approach outperforms the reactive approach

b	a	Full Info	High Info	Medium Info	Low Info	b	a	Full Info	High Info	Medium Info	Low Info
	1	80%	70%	66%	87%		1	57%	59%	64%	65%
	2	95%	75%	62%	71%		2	0%	0%	59%	61%
1.5	3	100%	73%	31%	0%	4.5	3	0%	0%	8%	28%
	4	100%	70%	15%	0%		4	0%	0%	0%	6%
	5	100%	65%	0%	0%		5	0%	0%	0%	0%
	1	77%	72%	75%	92%		1	0%	0%	0%	56%
	2	91%	85%	83%	91%		2	0%	0%	0%	0%
2.5	3	97%	89%	79%	84%	5.5	3	0%	0%	0%	0%
	4	100%	91%	76%	77%		4	0%	0%	0%	0%
	5	100%	91%	75%	73%		5	0%	0%	0%	0%
	1	70%	70%	76%	80%		1	0%	0%	0%	0%
	2	66%	69%	76%	82%		2	0%	0%	0%	0%
3.5	3	60%	65%	75%	86%	6.5	3	0%	0%	0%	0%
	4	21%	63%	77%	90%		4	0%	0%	0%	0%
	5	0%	53%	78%	93%		5	0%	0%	0%	0%

We conduct additional analyses with four clusters to assess the robustness of our results. We observe similar patterns in Table A.9: When repair demand is high relative to capacity ($b < 4$), the cyclic approach tends to perform better. As repair demand decreases relative to capacity ($b > 5$), the reactive approach becomes more effective.

Table A.9 Four Clusters: % of initial states where the cyclic approach outperforms the reactive approach

b	a	Full Info	High Info	Medium Info	Low Info	b	a	Full Info	High Info	Medium Info	Low Info
	1	30%	9%	1%	53%		1	45%	45%	58%	71%
	2	54%	8%	0%	0%		2	38%	42%	51%	62%
1.5	3	46%	5%	0%	0%	4.5	3	23%	36%	50%	69%
	4	46%	3%	0%	0%		4	14%	35%	53%	74%
	5	46%	2%	0%	0%		5	5%	32%	55%	77%
	1	60%	42%	35%	81%		1	26%	30%	37%	38%
	2	81%	57%	35%	56%		2	0%	8%	27%	32%
2.5	3	83%	56%	18%	19%	5.5	3	0%	0%	6%	19%
	4	83%	53%	11%	4%		4	0%	0%	2%	8%
	5	83%	46%	6%	2%		5	0%	0%	2%	5%
	1	54%	49%	56%	89%		1	0%	0%	6%	23%
	2	76%	68%	65%	82%		2	0%	0%	0%	0%
3.5	3	85%	70%	58%	67%	6.5	3	0%	0%	0%	0%
	4	87%	71%	54%	60%		4	0%	0%	0%	0%
	5	84%	71%	53%	55%		5	0%	0%	0%	0%

D.3.1. Analytical Derivation For better tractability, we consider full information, i.e., $q = 1$. We start with a likely initial state, defined as $s_0 = ((0,1),(\Omega_2, \Delta_2 = 3),(\Omega_3, \Delta_3 = 2))$, with $\Omega_2 > \Omega_3$. We consider two heuristic approaches - the cyclic approach visits the cluster with highest Δ and the reactive approach visits the cluster with the largest Ω. They differ in the visitation decision when the cluster with the largest Ω is not the same one with the highest Δ. Once the two approaches make different visitation decisions (i.e., they "split"), their states begin to diverge because they visit different clusters. However, at some future period the reactive approach may choose to visit the cluster with the highest Δ value as well (i.e., the cluster with the largest Ω is also the one with the highest Δ). When that happens, in the next period, the two approaches start with the same system state (i.e., of the three clusters, one cluster has $\Delta = 1$, one cluster has $\Delta = 2$, and one cluster has $\Delta = 3$), and from that point on the two approaches are effectively merged (i.e., identical action in the same period). The two processes are identical until the next split time. This means that we can view the comparison as a renewal-reward process on the split–merge intervals. The derivation therefore considers all possible periods from the first split up to the merging point, computing the conditional expected downtime differences over the divergent sample paths and weighting these differences by their respective probabilities. This approach captures the cumulative downtime during divergence while recognizing that once the two approaches merge, the subsequent evolution of the system does not contribute further to the difference in expected downtime.

We will write out all possible sample path under the reactive approach until period $t = 5$. There are eight possible sample paths that lead to $t = 5$. As t increases, there is an exponential increase in the number of possible sample paths, which makes the problem intractable. In addition, it is also unlikely that we need to go beyond period $t > 5$ because it is very unlikely that, under the reactive approach, we do not visit one particular cluster until period 6.

In $t = 1$, the system is at $s = (0,1),(\Omega_2, 3),(\Omega_3, 2)$. We assume $\Omega_2 > \Omega_3$. The expected downtime is $E[D_1] = \Omega_2 + \Omega_3$. The action is to visit cluster 2 under either the cyclic or reactive policy. In $t = 2$, $s = ((x,2),(0,1),(\Omega_3 + y_1, 3))$, with $x \sim \text{Bin}(W, p(1))$ and $y_1 \sim \text{Bin}(W - \Omega_3, p(2))$. The visitation decision is based on comparing x (from Cluster 1) and $\Omega_3 + y_1$ (from Cluster 3).

In $t = 3$, there are two cases. Case one is when $\Omega_3 + y_1 < x$, and the decision is to visit Cluster 1. Then, in $t = 3$ the system is updated as: $s = ((0,1),(x,2),(\Omega_3 + y_1 + y_2, 4))$, with $x \sim \text{Bin}(W, p(1))$ and $y_2 \sim \text{Bin}\big(W - (\Omega_3 + y_1),\, p(3)\big)$. Thus, the conditional expected water point downtime is: $E[D_3^a | x > \Omega_3 + y_1] = \sum_{x, y_1 : x > \Omega_3 + y_1} \Big(W p(1) + \Omega_3 + y_1 + \big(W - (\Omega_3 + y_1)\big) p(3)\Big) \cdot P(x, y_1) / P(x > \Omega_3 + y_1)$. The probability of choosing case 1 is $\theta_3 = \Pr\{x > \Omega_3 + y_1\}$. Case two is when $\Omega_3 + y_1 \geq x$, and both policies have the same visitation action.

In $t = 4$, since under the second case, the two policies match, leading to the same future water point downtime. Thus, with probability $1 - \theta_3$, we do not have to go down this path and can assume that the difference between the two policies' total expected downtime in a discounted infinite horizon is zero. Under the first case, there are two possibilities again. Case (a) is when $\Omega_3 + y_1 + y_2 < x$, and the Conditional expected downtime is $E[D_4^a | x > \Omega_3 + y_1 + y_2] = \sum_{x, y_1, y_2 : \atop x > \Omega_3 + y_1 + y_2} \Big(W\, p(1) + \big(\Omega_3 + y_1 + y_2\big) + \Big(W - \big(\Omega_3 + y_1 + y_2\big)\Big) p(4)\Big)\, P(x, y_1, y_2) / P(x > \Omega_3 + y_1 + y_2)$. Case (b) is when $\Omega_3 + y_1 + y_2 \geq x$, and the two policies take the same visitation action, leading to the same future water point downtime. And we can assume that the difference between the two policies' total expected downtime in a discounted infinite horizon is zero.

In case (a) the decision is deterministic based on the highest Ω, with $\theta_4 = \mathbf{1}\{x > \Omega_3 + y_1 + y_2\}$. Using summation form over the possible realizations:

$$\theta_4 = \sum_{x=0}^{W} \sum_{y_1=0}^{W-\Omega_3} \sum_{y_2=0}^{W-(\Omega_3+y_1)} \mathbf{1}\{x > \Omega_3 + y_1 + y_2\}\, P(x)\, P(y_1)\, P(y_2 \mid y_1),$$

$$\text{where } P(x) = \binom{W}{x} [p(1)]^x [1 - p(1)]^{W-x},\ P(y_1) = \binom{W - \Omega_3}{y_1} [p(2)]^{y_1} [1 - p(2)]^{W - \Omega_3 - y_1},$$
$$P(y_2 \mid y_1) = \binom{W - \Omega_3 - y_1}{y_2} [p(3)]^{y_2} [1 - p(3)]^{W - \Omega_3 - y_1 - y_2}.$$

In $t = 5$, under case (a) we have two cases again. Case (a1) is when $\Omega_3 + y_1 + y_2 + y_3 < x$, the NGO would visit cluster 1, and the state of the system is $((0,1),(x,2),(\Omega_3 + y_1 + y_2 + y_3 + y_4, 6))$, with $y_4 \sim \text{Bin}\Big(W - \Omega_3 - y_1 - y_2 - y_3, p(5)\Big)$. Conditional expected downtime:

$$E[D_5^a | x > \Omega_3 + y_1 + y_2 + y_3] = \frac{\sum\limits_{\substack{x, y_1, y_2, y_3 \\ x > \Omega_3 + y_1 + y_2 + y_3}} \Big(W\, p(1) + \big(\Omega_3 + y_1 + y_2 + y_3\big) + \big(W - (\Omega_3 + y_1 + y_2 + y_3)\big) p(5)\Big)\, P(x, y_1, y_2, y_3)}{P(x > \Omega_3 + y_1 + y_2 + y_3)}$$

As before, in case (a2), we have $\Omega_3 + y_1 + y_2 + y_3 > x$, and the two policies choose to visit the same cluster.

Throughout the periods, under a cyclic maintenance visitation approach, each cluster is visited every three periods. In $t = 1$, the downtime is $\Omega_3 + \Omega_2$. In $t = 2$, the downtime is $W \cdot p(1) + \Omega_3 + (W - \Omega_3) \cdot p(2)$. Starting in $t = 3$, the per period total downtime for all three clusters is the same: $D^c = D_t^c = 2W \cdot p(1) + W \cdot (1 - p(1)) \cdot p(2)$.

We can extend to infinite horizon,

$$E[D_\infty^r] - E[D_\infty^c] = \theta_3 \left\{ \Psi_3 + \sum_{t=4}^{\infty} \left(\prod_{k=4}^{t} \theta_k \right) \Psi_t \right\},$$

where $\theta_t = Pr\Big\{x > \Omega_3 + \sum_{j=1}^{t-2} y_j\Big\}; \Psi_t = E\Big[D_t^a \mid x > \Omega_3 + \sum_{j=1}^{t-2} y_j\Big] - D_t^c \quad (\forall t \geq 4), x \sim Bin(W, p(1))$; and $y_j \sim Bin\Big(W - \Omega_3 - \sum_{k=1}^{j-1} y_k, p(j+1)\Big)$, for $j = 1, 2.., t-2$.

To provide analytical insights into the structure of each policy, we can analytically show the existence of a threshold b such that for $b \geq b^\star$, the reactive policy's downtime decreases monotonically in b, while the cyclic policy's downtime is always monotonically decreasing in b. This insight also shows, albeit indirectly, that as b increases, the reactive policy may reach a lower downtime compared to the cyclic policy.

Note that θ_t is conditional on already having diverged, the reactive policy again picks a different cluster than the cyclic policy at the next step. As time progresses (i.e., as more y_i's are added), the cumulative value on the right-hand side increases, making it less likely that x continues to exceed this sum. In other words, the probability of sustained divergence decreases with each additional period. For example, when $a = 1$ and $b = 6.5$, $\theta_5 = 0.012$, and when $\Omega_3 = 0$, $a = 1$, and $b = 1.5$, we find $\theta_5 = 4.28 \times 10^{-6}$. Due to the infinite nested sums of binomial terms, it is not possible to derive simple closed form conditions under which one approach dominates the other. Therefore, we truncate the analysis at period 5, where the probability becomes negligible. The Final Difference at $t = 5$ is $E[D_5^r] - E[D_5^c] = \theta_3\Big(\Psi_3 + \theta_4\, \Psi_4 + \theta_4\, \theta_5\, \Psi_5\Big)$. Define

$$\theta_3 = \Pr\{x > \Omega_3 + y_1\}; \theta_4 = \Pr\{x > \Omega_3 + y_1 + y_2 | x > \Omega_3 + y_1\}; \theta_5 = \Pr\{x > \Omega_3 + y_1 + y_2 + y_3 | x > \Omega_3 + y_1 + y_2\},$$
$$\Psi_3 = E\Big[D_3^a \mid x > \Omega_3 + y_1\Big] - D_3^c; \Psi_4 = E\Big[D_4^a \mid x > \Omega_3 + y_1 + y_2\Big] - D_4^c; \Psi_5 = E\Big[D_5^a \mid x > \Omega_3 + y_1 + y_2 + y_3\Big] - D_5^c.$$

In order for $E[D_5^r] - E[D_5^c]$ to be negative, i.e., the reactive approach is preferred, we need

$$\begin{aligned} &\sum_{\substack{x, y_1: \\ x > \Omega_3 + y_1}} \Big(W\, p(1) + \Omega_3 + y_1 + [W - (\Omega_3 + y_1)] p(3)\Big) P(x) P(y_1) \\ &\quad + \theta_3 \sum_{\substack{x, y_1, y_2: \\ x > \Omega_3 + y_1 + y_2}} \Big(W\, p(1) + \big(\Omega_3 + y_1 + y_2\big) + \big(W - (\Omega_3 + y_1 + y_2)\big) p(4)\Big) P(x) P(y_1) P(y_2 \mid y_1) \\ &\quad + \theta_3\, \theta_4 \sum_{\substack{x, y_1, y_2, y_3: \\ x > \Omega_3 + y_1 + y_2 + y_3}} \Big(W\, p(1) + \big(\Omega_3 + y_1 + y_2 + y_3\big) + \big(W - (\Omega_3 + y_1 + y_2 + y_3)\big) p(5)\Big) \\ &\qquad \times P(x) P(y_1) P(y_2 \mid y_1) P(y_3 \mid y_1, y_2) \leq D^c\, \theta_3 \Big(1 + \theta_4 + \theta_4\, \theta_5\Big). \end{aligned} \tag{A.8}$$

Throughout the proof, we will use the following three properties:

(1) The probability $p(\Delta)$ is monotonically decreasing in b because $\frac{d}{db}\, p(\Delta) = -\,a\, p(\Delta)\big(1 - p(\Delta)\big)$.

(2) The binomial tail probabilities are monotonically decreasing in b, i.e., if $X \sim \text{Binomial}(n, p)$, then for any integer k, $\Pr(X > k)$ is an decreasing function of b. We show this below: Let $U_1, \ldots, U_n$ be i.i.d.

$\mathrm{Uniform}(0,1)$. For each $p \in [0,1]$, define $X(p) = \sum_{i=1}^{n} \mathbf{1}\{U_i < p\}$. Then $X(p) \sim \mathrm{Bin}(n,p)$. Moreover, if $p_1 < p_2$, then for each i, $\mathbf{1}\{U_i < p_1\} \le \mathbf{1}\{U_i < p_2\}$, and hence almost surely $X(p_1) \le X(p_2)$. It follows that for any integer k and any $p_1 < p_2$, $\{X(p_1) > k\} \subseteq \{X(p_2) > k\}$, we have $\Pr\big(X(p_1) > k\big) \le \Pr\big(X(p_2) > k\big)$. Therefore the tail probability $\Pr_{X\sim\mathrm{Bin}(n,p)}\big(X > k\big)$ is non-decreasing in p. Since p decreases in b, we have $\Pr(X > k)$ is monotonically decreasing in b.

(3) Let $y_1 \sim \mathrm{Bin}(W - \Omega_3, p(2))$ and define $P_{p(2)}(y_1) = \binom{W-\Omega_3}{y_1} p(2)^{y_1} \left(1-p(2)\right)^{W-\Omega_3-y_1}$. Then

$$\begin{aligned}
\frac{d}{db} P_{p(2)}(y_1) &= \frac{dP_{p(2)}(y_1)}{dp(2)} \, \frac{dp(2)}{db} \\
&= \binom{W-\Omega_3}{y_1} \Big[y_1 \, p(2)^{\,y_1-1} \, (1-p(2))^{\,W-\Omega_3-y_1} \; - \; (W-\Omega_3-y_1) \, p(2)^{\,y_1} \, (1-p(2))^{\,W-\Omega_3-y_1-1} \Big] \, \big(-a\, p(2)\,(1-p(2))\big) \\
&= -a\,(y_1 - (W-\Omega_3)\,p(2)) \, \binom{W-\Omega_3}{y_1} \, p(2)^{y_1} \, (1-p(2))^{\,W-\Omega_3-y_1} \\
&= -\,a\,\big(y_1 - (W-\Omega_3)\,p(2)\big) \, P_{p(2)}(y_1)\,.
\end{aligned}$$

When $y_1 > (W-\Omega_3)p(2)$, $P_{p(2)}(y_1)$ is monotonically decreasing in b.

We first analyze the first term on the left hand side of Equation (A.8):

$$\begin{aligned}
H(b) &= \sum_{\substack{x,y_1:\\ x>\Omega_3+y_1}} \Big(W\,p(1) + \Omega_3 + y_1 + \big[W - (\Omega_3+y_1)\big]\,p(3) \Big) P_{p(1)}(x) P_{p(2)}(y_1) \\
&= \sum_{y_1=0}^{W-\Omega_3} \Big(W\,p(1) + \Omega_3 + y_1 + \big[W - (\Omega_3+y_1)\big]\,p(3) \Big) P_{p(2)}(y_1) \sum_{x=\Omega_3+y_1+1}^{W} P_{p(1)}(x) \\
&= \sum_{y_1=0}^{W-\Omega_3} F(y_1)\, P_{p(2)}(y_1) \Phi\big(y_1;\, p(1)\big),
\end{aligned}$$

where $F(y_1) = W\,p(1) + \Omega_3 + y_1 + \big[W - (\Omega_3+y_1)\big]\,p(3)$, and $\Phi\big(y_1;\,p(1)\big) = \sum_{x=\Omega_3+y_1+1}^{W} P_{p(1)}(x)$.

Differentiate term-by-term using the product rule:

$$\begin{aligned}
H'(b) &= \sum_{y_1=0}^{W-\Omega_3} \Big[\tfrac{(y_1)}{\partial b} \, P_{p(2)}(y_1)\,\Phi \; + \; F(y_1) \, \tfrac{d}{db} P_{p(2)}(y_1)\,\Phi + \; F(y_1)\, P_{p(2)}(y_1) \, \tfrac{d}{db} \Phi\big(y_1;p(1)\big) \Big] \\
&= \sum_{y_1=0}^{W-\Omega_3} \Big[\big(W\,p_1' + (W-\Omega_3-y_1)\,p_3'\big)\, P_{p(2)}(y_1)\,\Phi(y_1;p_1) - a\,F(y_1)\,(y_1 - (W-\Omega_3)\,p_2)\,P_{p(2)}(y_1)\,\Phi(y_1;p_1) + \; F(y_1)\,P_{p(2)}(y_1)\,\Phi_p\big(y_1;p_1\big)\,p_1' \Big].
\end{aligned}$$

Let us now analyze the signs of each term. For the first term, because $p_1' < 0$, $p_3' < 0$, $P_{p(2)}(y_1) > 0$, $\Phi(y_1;p_1) > 0$, we have $\big(W\,p_1' + (W-\Omega_3-y_1)\,p_3'\big)\, P_{p(2)}(y_1)\,\Phi(y_1;p_1) \le 0$.

For the third term, because $F(y_1) > 0$, $P_{p(2)}(y_1) > 0$, $\Phi_p(y_1;p_1) > 0$, $p_1' < 0$, we have $F(y_1)\,P_{p(2)}(y_1)\,\Phi_p\big(y_1;p_1\big)\,p_1' \le 0$.

For the second term, when $y_1 \ge (W-\Omega_3)\,p_2$, we have $-a\,F(y_1)\,(y_1 - (W-\Omega_3)\,p_2)\,P_{p(2)}(y_1)\,\Phi(y_1;p_1) \le 0$. And when $y_1 < (W-\Omega_3)\,p_2$, we have $-a\,F(y_1)\,(y_1 - (W-\Omega_3)\,p_2)\,P_{p(2)}(y_1)\,\Phi(y_1;p_1) > 0$. Note that, as $b \to +\infty$, we have $p_2(b) \to 0$, so $(W-\Omega_3)p_2(b) \to 0$.

Because y_1 ranges over the finite set $\{1,\ldots,W-\Omega_3\}$, there exists a finite $b^* = \max_{0\le y_1\le W-\Omega_3}\Big\{ b : y_1 = (W-\Omega_3)\,p_2(b) \Big\}$ such that for all $b \ge b^*$ one has $y_1 \ge (W-\Omega_3)\,p_2(b)$ for every $y_1 \in \{1,\ldots,W-\Omega_3\}$. Note when $y_1 = 0$, the second term is 0 and thus trivial.

So, now we have established that there exists a finite threshold b^* such that $H'(b) < 0$ for all $b \ge b^*$. In other words, $H(b)$ ultimately decreases as b grows large.

For the second and third term on the left hand-side, we can use a similar logic to show that each ultimately decreases as b grows large. Due to space constraint, we ultimately omit them here.

Lastly, from property (2), we know that each θ_t is monotonically decreasing in b. From property (1), we know that $D^c = D_t^c = 2W \cdot p(1) + W \cdot (1-p(1)) \cdot p(2)$ is also monotonically decreasing in b.

To summarize the proof, we have shown that there exists a threshold b^* such that all the terms on the left hand side of the boxed equation is monotonically decreasing in b. We have also shown that the right hand side of the boxed equation is always monotonically decreasing in b.

D.4. Convex Increasing Downtime Cost

For each cluster i, we define a histogram vector $\mathbf{l}_{i,t} = \Big(l_{i,t}(1), l_{i,t}(2), \ldots, l_{i,t}(J)\Big)$, where $l_{i,t}(j)$ is the number of water points in cluster i that have been broken for exactly j periods. The augmented state is then $s_{it} = \Big(\Delta_{it}, \mathbf{l}_{i,t}\Big)$, with the total number of broken water points given by $\Omega_{it} = \sum_{j=1}^{J} l_{i,t}(j)$.

If the cluster is visited ($a_{it} = 1$), then $l_{i,t+1}(j) = 0$, $\forall\, j = 1, \ldots, J$, $\Delta_{i,t+1} = 1$.

If the cluster is not visited ($a_{it} = 0$), then $\Delta_{i,t+1} = \Delta_{it} + 1$, and

$$l_{i,t+1}(j+1) = l_{i,t}(j), j = 1, \ldots, J-1, l_{i,t+1}(1) = h, \text{with } h \sim \text{Bin}\Big(W_i - \sum_{j=1}^{J} l_{i,t}(j),\, p(\Delta_{it}) \cdot q\Big).$$

Let $f : \mathbb{N} \to \mathbb{R}_+$ be a convex, increasing function of $f(j) = j^2$. The downtime cost for cluster i is then $\sum_{j=1}^{J} f(j)\, l_{i,t}(j)$. The modified per-period cost function becomes $g(\mathbf{s}_t, \mathbf{a}_t) = \alpha \cdot (\text{Logistics cost}) + (1-\alpha) \cdot \sum_{i=1}^{N_c} \sum_{j=1}^{J} f(j)\, l_{i,t}(j)$.

We conduct a numerical experiment with generated data of $N_c = 3$ clusters, each with $W = 10$ water points, over six periods. We set $a = 1$ to model a relatively smooth increase as Δ increases. As in our previous experiments, we examine a range of b values from $\{1.5, 2.5, ..., 6.5\}$. We set $\alpha = 0$ (i.e., we only consider downtime cost) and $q = 1$ (i.e., full information). We run the model with our original objective function, which minimizes cumulative downtime days, and the alternative formulation of a convex increasing downtime cost.

Under our original objective function, i.e., minimizing total accumulated downtime days, we find that as b increases from 1.5 to 6.5, the percentage of initial states where the optimal action targets the cluster with the highest Δ decreases significantly, from 85.12% to 61.12%. In contrast, the percentage of initial states where the optimal action targets the cluster with the highest Ω increases significantly, from 71.19% to 95.20%. These results are consistent with our cyclic vs. reactive maintenance visitation approach comparisons (presented in Section 5.3), suggesting that when repair demand is relatively low compared to NGO capacity, the reactive approach that targets the cluster with the highest Ω performs better.

In contrast, under the convex downtime cost objective, the decision rule remains stable across different values of b. As b increases from 1.5 to 6.5, the frequency of selecting the cluster with the highest Δ, across all initial states, remains nearly constant (from 75.66% to 75.82%). Moreover, we find that the dominant strategy is to visit the cluster with the highest weighted downtime, which is defined as the sum over all downtime periods (from 1 to 6) of the product of the number of broken water points and the corresponding period count. This strategy, which is chosen on average 93.57% of the time across different b values.

Overall, these findings indicate that the structure of the downtime cost function may influence the optimal decision-making policy. Under the original formulation based on downtime days, the focus shifts toward clusters with higher repair needs as capacity increases. In contrast, the convex formulation yields a more balanced and stable decision pattern even as capacity varies. Given that actual downtime costs are affected by numerous factors, such as economic conditions (with poorer communities being disproportionately affected) and water quality, the availability of alternative water sources (e.g., surface water, rain), which are all difficult to quantify objectively, we have chosen to use the operational metric of downtime days for our main analysis.

References

Carter R (2021) *Rural Community Water Supply: Sustainable Services for All* (United Kingdom: Practical Action Publishing).

Erpf K (2007) *Installation and Maintenance Manual for the Afridev Handpump (Revision 2–2007)*. Rural Water Supply Network (RWSN) / SKAT, St. Gallen, Switzerland, URL `https://www.pseau.org/outils/ouvrages/skat_afridev_installation_and_maintenance_manual_2007.pdf`, accessed: 2024-08-12.

Wilson DJ (2019) The harmonic mean p-value for combining dependent tests. *Proceedings of the National Academy of Sciences USA* 116(4):1195–1200.